Segmentation of B_1 Inhomogeneity MR Brain Image Using Mixture Gaussian Model and Markov Random Field

Z. Peng[1], W. Wee[1], J. Zhong[1], J-H. Lee[2]

[1]Electrical & Computer Engineering and Computer Science, University of Cincinnati, Cincinnati, Ohio, United States, [2]Bidmedical Engineering, University of Cincinnati, Cincinnati, Ohio, United States

Introduction

The segmentation of MR brain imaging has significant applications in brain morphometric studies. There are a large number of approaches for MR brain image and/or surface segmentation methods that include edge detection and segmentation[1], classification methods[2], region growing methods[3], and deformable contour and surface methods[4]. Most of these methods are based on an assumption that the intensities of each tissue class are relatively constant. However, this assumption is not true for high-field MR images (> 3T) due to severe B_1 inhomogeneity. This non-uniformity may produce up to 30% variation of image intensity [5] and is especially severe for ultra high-field MR system (>7T). Although this problem may be alleviated by using some correction techniques, how to accurately model the inhomogeneities distribution is still an open question. Most of above image segmentation approaches fail to provide accurate results. In this paper we will show a novel approach to improve segmentation accuracy by designing a learning mechanism to recognize the radiologists segmented results and also derive an algorithm to adapt the learned information to the slowly changes of the sequential (adjacent) image in an automatic manner.

Methods

MR brain images were generated from a 4T Varian whole body MRI system using the MDEFT 3D imaging sequence [6]. Markov models were employed to derive a recursive algorithm for computing the maximum a posteriori probability (**MAP**) $p(\omega | I(x,y)) \propto p(I(x,y)|\omega)p(\omega)$, where $\omega \in \{\omega_1, \omega_2, \omega_3\}$ denoted the tissue assignment, and $I(x,y)$ was the image intensity at position (x,y). In many applications, the conditional class probability distribution $p(I(x,y)|\omega)$ was modeled by a single Gaussian distribution. In here, for the image intensity inhomogeneity, we modeled it by a mixture Gaussian model with N mean vectors, where $N = N_1 + N_2 + N_3$ denoted the total number of mean vectors (or cluster centers) with N_1, N_2, and N_3 centers in WM, GM, and CSF, respectively. The priori probability $p(\omega)$ model was based on a 2-D Markov Random Field (**MRF**) [7]. Then, we designed a learning mechanism that learned from an MR brain image that had been segmented into WM, GM, and CSF regions provided by radiologists. The learning mechanism consists of two major parts: i) the learning process and ii) the verification process. Firstly, the learning process uses a modified K-mean (**MKM**) algorithm to do knowledge abstraction and representation. In order to make sure that all learned cluster centers were located within the region of their representations, we used the adaptive sample set construction (**ASSC**) [8] algorithm to increase the number of centers for each erroneously designated center until no erroneously designated centers existed. Secondly, the verification process was applied to verify the validity of the learned knowledge using a **MRF** decision algorithm operating on the same image. Then, with the resulting learned cluster centers and parameter settings, we applied the **MRF** decision algorithm to the subsequence MR brain images to obtain the segmentation results. Furthermore, an adaptive algorithm was also provided to adjust the learned knowledge to the slowly varying subsequent MR brain images sequentially all in an automatic manner without human intervention.

Results

The MR images were first preprocessed by MRIcro (www.mricro.com) to eliminate the skull. Figures 1(a)–(d) show the original image, radiologists manually drawn segmentation, the position of WM cluster centers (blue dots) for the learning mechanism and the segmentation results using the proposed algorithm, respectively. The accuracy of the results compared with the radiologists' manually drawn segmentation is 93.3%(WM), 92.0%(GM), and 90.3%(CSF). The segmentation accuracy of the artificial shifted MR image is listed in Table 1. Figures 2 (a) and (b) show one of original subsequent image slices (3 mm off the trained slice) and its segmentation result by using adaptive learning algorithm with accuracy of 90.9%(WM), 84.4%(GM) and 82.8%(CSF) .

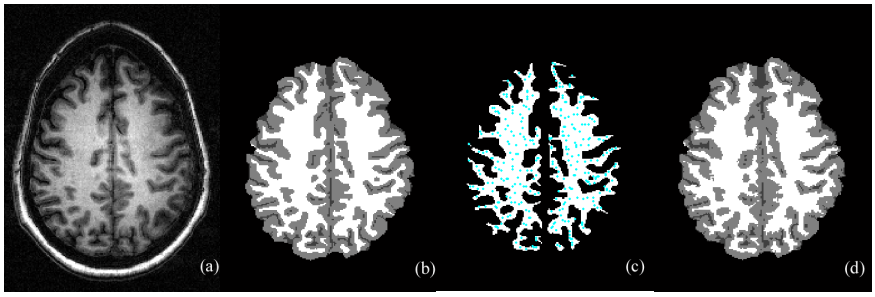

Figure 1 (a) original MR image, (b) radiologists drawn segmentation, (c) the position of WM mean vector centers, (d) the segmentation result using our methods.

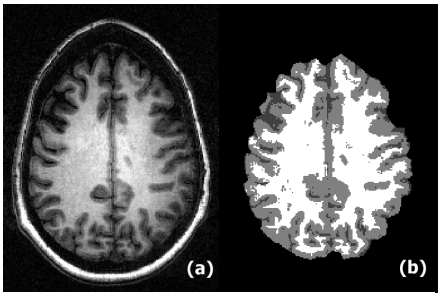

Figure 2 (a) one of original subsequence images (b) segmentation result

Shift pixels	1	2	3	4	5	6	7	8	9	10
WM	93.8%	93.6%	93.0%	91.8%	90.5%	89.4%	87.7%	86.2%	85.2%	84.9%
GM	92.1%	91.8%	90.8%	90.1%	89.1%	87.9%	86.5%	86.0%	84.6%	84.4%
CSF	90.3%	90.7%	90.8%	89.5%	88.2%	86.4%	84.2%	82.2%	79.5%	78.3%

Table 1. The accuracy of segmentation results of the artificial shifted MR image.

Discussion/Conclusion

In this paper, we provide a new MR brain segmentation scheme using the mixture Gaussian Model and MRF, which is less sensitive to the B_1 inhomogeneity. The preliminary results showed that our method provided a highly accurate and robust mechanism to duplicate WM, GM, and CSF provided by the radiologists and could be used to improve the performance of subsequence image segmentation.

As shown in Table 1 and Figure 2, the segmentation of CSF is less robust than that of WM and GM. This larger amount of misclassification is mainly due to its extremely complex structure in cortical sulci. Our future work will concentrate on more powerful learning algorithm that can describe complex matters such as CSF more precisely.

References

[1] Bomans M, Hohne K, Tiede U, Riemer M, *IEEE Trans. Med. Imag.*, **9**, 177-183, 1990.

[2] Rajapakse JC, Giedd JN, Rapoport JL, *IEEE Trans. Med. Imag.*, **16**, 176-186, 1997.

[3] Hata Y, Kobashi S, Hirano S, Kitagaki H, Mori E, *IEEE Trans. Syst., Man., and Cybern C*, **30**, 381-395, 2000.

[4] Zeng X, Staib LH, Schultz RT, Duncan JS, *IEEE Trans. Med. Imag.*, **18**, 927-937, 1999.

[5] Meyer CR, Hland PH, Pipe J, *IEEE Trans. Med. Imag.*, **14**, 36-41, 1995.

[6] Lee J-H, Garwood M, Menon R, Adriany G, Anderson P, Truwit CL, Ugurbil K. *MRM* **34**, 308-312, 1995.

[7] Geman D, Geman S, Graffigne C, Dong P, *IEEE Trans. Pattern Anal. Machine Intell.*, **12**, 609-628, 1990.

[8] Sebestyen, G.S, Procedings FJCC, 685-694, 1966.